ISSN 0025-6544, Mechanics of Solids, 2022, Vol. 57, No. 7, pp. 1781–1792. © Allerton Press, Inc., 2022.
Russian Text © The Author(s), 2022, published in Prikladnaya Matematika i Mekhanika, 2022, Vol. 86, No. 2, pp. 263–275.

Stress-Strain State of a Shallow Tunnel Supported by a Three-Layer Shell Affected by Transport Loads

L. A. Alexeyeva[a],*, V. N. Ukrainets[b],, and S. R. Girnis[b],*****

[a] *Institute of Mathematics and Mathematical Modeling, Almaty, 050010 Kazakhstan*

[b] *Toraighyrov University, Pavlodar, 140008 Kazakhstan*

**e-mail: alexeeva@math.kz*

***e-mail: ukrainets.v@teachers.tou.edu.kz*

****e-mail: girnis.s@teachers.tou.edu.kz*

Received August 10, 2021; revised January 20, 2022; accepted January 25, 2022

Abstract—The problem of the effect of a load moving at a constant velocity over a three-layer circular cylindrical shell in an elastic half-space is solved. The dynamic equations of the elasticity theory in the Lamé potentials are used to describe the motion of the half-space and the inner layer of the shell. Oscillations of the outer layers of the shell are described based on the classical equations of the theory of thin shells. The solution has been obtained for the case when the velocity of the load is less than the velocity of the Rayleigh wave and the critical velocities of the latter. Based on the solution of the problem, the stress-strain state is studied for a shallow tunnel reinforced with the use of a three-layer steel-concrete lining affected by a symmetric or asymmetric normal load originating from the intratunnel transport uniformly moving along its tray.

Keywords: tunnel, elastic half-space, three-layered shell, moving load, stress-strain state

DOI: 10.3103/S0025654422070032

1. INTRODUCTION

One of the model problems used in the studies on the dynamics of shallow tunnels affected by transport load (the load originating from a moving intratunnel transport) is represented by a problem of the effect of a load uniformly moving on the inner shell surface along its generatrix parallel to a free half-space boundary. In contrast to a similar problem for an elastic space that simulates a deep tunnel, this problem is more complicated, since it becomes necessary to take into account the waves reflected by the boundary of the half-space. Therefore, the number of publications devoted to the studies on this problem is not numerous and covers mainly recent years, see, in particular, [1–8].

In the present study, a mathematical model for the dynamics of a shallow tunnel reinforced with a three-layer lining affected by a traffic load is constructed. Using the method of incomplete variable separation and re-expansion of cylindrical and plane waves, an analytical solution of the problem has been constructed based on which an algorithm is developed and a software package in the FORTRAN language is developed in order to calculate the stress-strain state of the tunnel lining and rock body, taking into account the velocity of the traffic load, the depth of the tunnel, and the physicomechanical properties of the body and the material of the shells. A subsonic case is considered, wherein the motion velocity is less than the propagation velocity of elastic waves in the body, including the Rayleigh wave velocity for an elastic half-space. The results of numerical experiments are presented and analyzed.

2. PROBLEM FORMULATION AND ANALYTICAL SOLUTION

As a design scheme for a shallow tunnel reinforced with a three-layer lining, an infinitely long circular cylindrical three-layered shell is considered in a linearly elastic, homogeneous and isotropic half-space (body) referred to as fixed cylindrical r, θ, z and Cartesian x, y, z coordinate systems, whose axis coincides with the axis of the shell and is parallel to the load-free horizontal boundary of the half-space (Earth's surface), the x-axis being perpendicular to this boundary: $x \le h$ (Fig. 1).

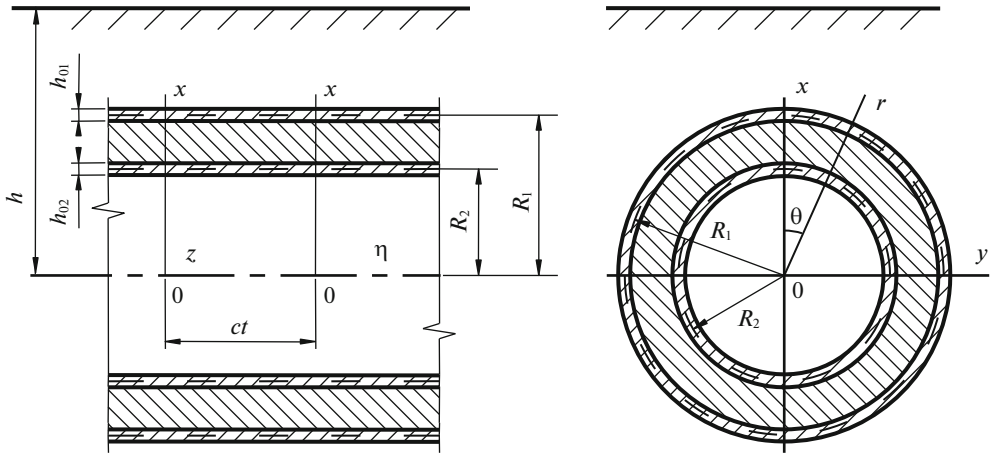

Fig. 1. Three-layer shell in an elastic half-space.

The inner layer of the shell represents a thick-walled shell (aggregate), whereas the outer layers (sheathing) consist of thin-walled shells with median surface radii R_1, R_2, and thicknesses h_{01}, h_{02}. Owing to the smallness of the layer thickness composing the sheathing, it is assumed that they are in contact with the aggregate and the surrounding body throughout their median surfaces. The contact between the layers of the shell is assumed to be rigid, whereas the contact between the shell and the body is assumed to be either rigid or sliding under a two-way connection in the radial direction.

On the inner surface of the shell in the direction of its z-axis at constant speed c moves a load with intensity P the form of which does not change over time (steady-state load). The motion velocity of the load is assumed subsonic, i.e., lower than the velocities of shear wave propagation in the aggregate and in the body (typical for modern vehicles). The physicomechanical properties of the body and aggregate are characterized, respectively, by the following constants: ν_1, μ_1, ρ_1; ν_2, μ_2, ρ_2, where ν_k is Poisson's ratio, μ_k is the shear modulus, and ρ_k is the density ($k = 1,2$). Further, index $k = 1$ refers to the body, whereas index $k = 2$ refers to the aggregate.

Since a steady-state process is considered, the deformation pattern is steady-state with respect to the moving load. Therefore, one can switch to a load-related moving a Cartesian $(x, y, \eta = z - ct)$ or cylindrical $(r, \theta, \eta = z - ct)$ coordinate system.

In order to describe the motion of the body and the aggregate, the following dynamic equations of the elasticity theory in a moving coordinate system are used [4]

$$(M_{pk}^{-2} - M_{sk}^{-2})\,\mathrm{grad}\,\mathrm{div}\,\mathbf{u}_k + M_{sk}^{-2}\nabla^2\mathbf{u}_k = \partial^2\mathbf{u}_k/\partial\eta^2, \quad k = 1,2, \tag{2.1}$$

where $M_{pk} = c/c_{pk}$, $M_{sk} = c/c_{sk}$ are the Mach numbers; $c_{pk} = \sqrt{(\lambda_k + 2\mu_k)/\rho_k}$, $c_{sk} = \sqrt{\mu_k/\rho_k}$ are the propagation velocities of expansion–compression and shear waves in the body and aggregate, $\lambda_k = 2\mu_k\nu_k/(1 - 2\nu_k)$; $\mathbf{u}_k$; are the displacement vectors of the body and aggregate points, and ∇^2 is the Laplace operator.

The oscillations of the sheathing layers can be described according to the classical equations of the theory of thin shells in a moving coordinate system, as it follows [2–4]

$$\left[1 - \frac{(1-\nu_{0k})\rho_{0k}c^2}{2\mu_{0k}}\right]\frac{\partial^2 u_{0\eta k}}{\partial\eta^2} + \frac{1-\nu_{0k}}{2R_k^2}\frac{\partial^2 u_{0\eta k}}{\partial\theta^2} +$$
$$+ \frac{1+\nu_{0k}}{2R_k}\frac{\partial^2 u_{0\theta k}}{\partial\eta\partial\theta} + \frac{\nu_{0k}}{R_k}\frac{\partial u_{0rk}}{\partial\eta} = \frac{1-\nu_{0k}}{2\mu_{0k}h_{0k}}\left(q_{\eta k} - q_{\eta R_k}\right),$$

$$\frac{1+\nu_{0k}}{2R_k}\frac{\partial^2 u_{0\eta k}}{\partial\eta\partial\theta}+\frac{(1-\nu_{0k})}{2}\left(1-\frac{\rho_{0k}c^2}{\mu_{0k}}\right)\frac{\partial^2 u_{0\theta k}}{\partial\eta^2}+$$
$$+\frac{1}{R_k^2}\frac{\partial^2 u_{0\theta k}}{\partial\theta^2}+\frac{1}{R_k^2}\frac{\partial u_{0rk}}{\partial\theta}=\frac{1-\nu_{0k}}{2\mu_{0k}h_{0k}}\left(q_{\theta k}-q_{\theta R_k}\right),$$
$$\frac{\nu_{0k}}{R_k}\frac{\partial u_{0\eta k}}{\partial\eta}+\frac{1}{R_k^2}\frac{\partial u_{0\theta k}}{\partial\theta}+\frac{h_{0k}^2}{12}\nabla^2\nabla^2 u_{0rk}+$$
$$+\frac{(1-\nu_{0k})\rho_{0k}c^2}{2\mu_{0k}}\frac{\partial^2 u_{0rk}}{\partial\eta^2}+\frac{u_{0rk}}{R_k^2}=-\frac{1-\nu_{0k}}{2\mu_{0k}h_{0k}}\left(q_{rk}-q_{rR_k}\right). \tag{2.2}$$

Here, for outer sheathing layer $k=1$, and for the inner one $k=2$; ν_{0k}, μ_{0k}, and ρ_{0k} are Poisson's ratio, the shear modulus, and the density of sheathing layer materials, respectively, $u_{0\eta k}$, $u_{0\theta k}$, and u_{0rk} are the displacements of the points of the midsurfaces of sheathing layers, $q_{jR_2}=\sigma_{rj2}\big|_{r=R_2}$, $q_{j1}=\sigma_{rj2}\big|_{r=R_1}$, and $q_{jR_1}=\sigma_{rj1}\big|_{r=R_1}$ are the components of the aggregate and body response, (under sliding contact between the shell and body $q_{\eta R_1}=q_{\theta R_1}=0$), σ_{rj1}, σ_{rj2} are the stress tensor components in the body and the aggregate, and $q_{j2}=P_j(\theta,\eta)$, $P_j(\theta,\eta)$ are the components of moving load intensity $P(\theta,\eta)$, $j=\eta,\theta,r$.

Since the boundary of the half-space is free from loads, then at $x=h$,

$$\sigma_{xx1}=\sigma_{xy1}=\sigma_{x\eta1}=0. \tag{2.3}$$

Under different contact conditions of the contact between the shell and the body, the boundary conditions have the following form:

– For a sliding contact between the shell and the body

$$\begin{gathered}\text{at}\quad r=R_1\quad u_{r1}=u_{r2},\quad u_{j2}=u_{0j1},\quad \sigma_{r\eta1}=0,\quad \sigma_{r\theta1}=0\\ \text{at}\quad r=R_2\quad u_{j2}=u_{0j2};\quad j=r,\theta,\eta;\end{gathered} \tag{2.4}$$

– For a rigid contact between the shell and the body

$$\begin{gathered}\text{at}\quad r=R_1\quad u_{j1}=u_{j2},\quad u_{j1}=u_{0j1}\\ \text{at}\quad r=R_2\quad u_{j2}=u_{0j2},\quad j=r,\theta,\eta,\end{gathered} \tag{2.5}$$

where u_{jk} are the components of vectors $\mathbf{u}_k$, $k=1,2$.

Vectors $\mathbf{u}_k$ can be expressed based on Lamé potentials [1, 4]

$$\mathbf{u}_k=\operatorname{grad}\varphi_{1k}+\operatorname{rot}\left(\varphi_{2k}\mathbf{e}_\eta\right)+\operatorname{rot}\operatorname{rot}\left(\varphi_{3k}\mathbf{e}_\eta\right);\quad k=1,2, \tag{2.6}$$

which, as it follows from (2.1) and (2.6), satisfy the following equations

$$\nabla^2\varphi_{jk}=M_{jk}^2\,\partial^2\varphi_{jk}\big/\partial\eta^2;\quad j=1,2,3,\quad k=1,2. \tag{2.7}$$

Here, $\mathbf{e}_\eta$ is the unit vector of the η-*axis*, $M_{1k}=M_{pk}$, $M_{2k}=M_{3k}=M_{sk}$.

Based on the same potentials, by using (2.6) and Hooke's law, one can express stress tensor components σ_{lmk} in the body ($k=1$) and in the aggregate ($k=2$) in the cylindrical coordinate system $(l,m=r,\theta,\eta)$, as well σ_{lm1} in the Cartesian coordinate system $(l,m=x,y,\eta)$.

Thus, in order to determine the components of the stress-strain state (SSS) for the body and for the aggregate, it is necessary to solve Eqs. (2.7) by using boundary conditions (2.3) and depending on the condition of contacting between the shell and the body, (2.4) or (2.5).

Let us consider the case of a shell affected by a sinusoidal (with respect to η) moving load arbitrarily depending on angular coordinate

$$P(\theta,\eta)=p(\theta)e^{i\xi\eta},\quad p(\theta)=\sum_{n=-\infty}^{\infty}P_n e^{in\theta},$$
$$P_j(\theta,\eta)=p_j(\theta)e^{i\xi\eta},\quad p_j(\theta)=\sum_{n=-\infty}^{\infty}P_{nj}e^{in\theta};\quad j=r,\theta,\eta, \tag{2.8}$$

where constant ξ determines period $T = 2\pi/\xi$ for acting load.

Under steady-state conditions, all quantities depending on η can be expressed according to (2.8), therefore

$$\phi_{jk}(r,\theta,\eta) = \Phi_{jk}(r,\theta)e^{i\xi\eta}; \quad j = 1, 2, 3, \quad k = 1, 2, \tag{2.9}$$

$$u_{0jk}(\theta,\eta) = \sum_{n=-\infty}^{\infty} u_{0njk}e^{in\theta}e^{i\xi\eta}; \quad j = r,\theta,\eta, \quad k = 1,2. \tag{2.10}$$

By substituting (2.9) into (2.7), one can obtain

$$\nabla_2^2\Phi_{jk} - m_{jk}^2\xi^2\Phi_{jk} = 0; \quad j = 1,2,3, \quad k = 1,2, \tag{2.11}$$

where $m_{jk} = (1 - M_{jk}^2)^{1/2}$, $m_{1k} = m_{pk}$, $m_{2k} = m_{3k} = m_{sk}$, ∇_2^2 is the two-dimensional Laplace operator.

By using (2.9), one can obtain relationships for displacements u_{lk}^* and stresses σ_{lmk}^* $(l,m = r,\theta,\eta)$ in the body ($k = 1$) and in the aggregate ($k = 2$), as well as u_{l1}^*, σ_{lm1}^* $(l,m = x,y,\eta)$ in the body depending on sinusoidal load as a function of Φ_{jk} (the * sign means that these components have been found for the shell affected by a sinusoidal moving load).

In the case of subsonic load velocity $M_{sk} < 1$, $m_{sk} > 0$, $k = 1,2$, and the solutions of Eqs. (2.11) can be represented [3, 4] in the following form

$$\Phi_{jk} = \Phi_{jk}^{(1)} + \Phi_{jk}^{(2)}, \quad j = 1,2,3, \quad k = 1,2, \tag{2.12}$$

where:

for the body

$$\Phi_{j1}^{(1)} = \sum_{n=-\infty}^{\infty} a_{nj}K_n(k_{j1}r)e^{in\theta}, \quad \Phi_{j1}^{(2)} = \int_{-\infty}^{\infty} g_j(\xi,\zeta)\exp(iy\zeta + (x-h)\sqrt{\zeta^2 + k_{j1}^2})d\zeta \tag{2.13}$$

and for the aggregate

$$\Phi_{j2}^{(1)} = \sum_{n=-\infty}^{\infty} a_{nj+3}K_n(k_{j2}r)e^{in\theta}, \quad \Phi_{j2}^{(2)} = \sum_{n=-\infty}^{\infty} a_{nj+6}I_n(k_{j2}r)e^{in\theta}. \tag{2.14}$$

Here, $I_n(k_jr)$, $K_n(k_jr)$, respectively, are the modified Bessel functions and Macdonald functions $k_{j1} = |m_{j1}\xi|$, $k_{j2} = |m_{j2}\xi|$; $g_j(\xi,\zeta)$, $a_{n1},\ldots,a_{n9}$, unknown functions, and coefficients to be determined, $j = 1,2,3$.

As it has been shown in [1, 2, 4], the representation of potentials for a half-space according to (2.12) leads to the following relationships for these potentials in the Cartesian coordinate system:

$$\Phi_{j1} = \int_{-\infty}^{\infty}\left[\frac{e^{-xf_j}}{2f_j}\sum_{n=-\infty}^{\infty} a_{nj}\Phi_{nj} + g_j(\xi,\zeta)e^{(x-h)f_j}\right]e^{iy\zeta}d\zeta, \tag{2.15}$$

where $f_j = \sqrt{\zeta^2 + k_{j1}^2}$, $\Phi_{nj} = \left[(\zeta + f_j)/k_{j1}\right]^n$; $j = 1,2,3$.

Let us use boundary conditions (2.3) rewritten for σ_{xx1}^*, σ_{xy1}^*, $\sigma_{x\eta1}^*$ taking into account (2.15). By separating the coefficients at $e^{iy\zeta}$ and equating them to zero, owing to the arbitrariness of y, one obtains a system of three equations, based on which one can express functions $g_j(\xi,\zeta)$ through unknown coefficients a_{n1}, a_{n2}, a_{n3}:

$$g_j(\xi,\zeta) = \frac{1}{\Delta^*}\sum_{l=1}^{3}\Delta_{jl}^*e^{-hf_l}\sum_{n=-\infty}^{\infty} a_{nl}\Phi_{nl}. \tag{2.16}$$

The form of determinant Δ^* and of algebraic complements Δ_{jl}^* coincides with similar determinants for an unsupported cavity in an elastic half-space and is determined in [2, 4]. In particular, here Δ^* is the Rayleigh determinant that in this case has the following form

$$\Delta^* = \left(2\rho_*^2 - \beta^2\right)^2 - 4\rho_*^2\sqrt{\rho_*^2 - \alpha^2}\sqrt{\rho_*^2 - \beta^2};$$

$$\alpha = M_{p1}\xi, \quad \beta = M_{s1}\xi, \quad \rho_*^2 = \xi^2 + \zeta^2,$$

and does not go to zero at any ζ, if the motion velocity of the load is less than Rayleigh surface wave velocity c_R, further called the Rayleigh velocity. Otherwise, it the determinant goes to zero at points $\zeta = \pm\zeta^* = \pm|\xi|\sqrt{M_R^2 - 1}$, $M_R = c/c_R$, and the integrals in relationship (2.15) become divergent.

Let's confine ourselves to a case where $c < c_R$. Then, all the integrands in (2.15) are continuous and tend to zero exponentially at infinity. Taking into account (2.16), potentials (2.15) have the following form

$$\Phi_{j1} = \int_{-\infty}^{\infty}\left[\frac{e^{-xf_j}}{2f_j}\sum_{n=-\infty}^{\infty}a_{nj}\Phi_{nj} + e^{(x-h)f_j}\sum_{l=1}^{3}\frac{\Delta_{jl}^*}{\Delta^*}e^{-hf_l}\sum_{n=-\infty}^{\infty}a_{nl}\Phi_{nl}\right]e^{iy\zeta}d\zeta. \tag{2.17}$$

It should be noted that Rayleigh velocity c_R is somewhat lower than the velocity of shear waves in the rock body.

Using the following relationship known for the case of $x < h$ [1, 2]

$$\exp(iy\zeta + (x-h)\sqrt{\zeta^2 + k_j^2}) = \sum_{n=-\infty}^{\infty}I_n(k_j r)e^{in\theta}[(\zeta + \sqrt{\zeta^2 + k_j^2})/k_j]^n e^{-h\sqrt{\zeta^2+k_j^2}},$$

let us represent Φ_{j1} (2.12) in a cylindrical coordinate system

$$\Phi_{j1} = \sum_{n=-\infty}^{\infty}\left(a_{nj}K_n(k_{j1}r) + I_n(k_{j1}r)\int_{-\infty}^{\infty}g_j(\xi,\zeta)\Phi_{nj}e^{-hf_j}d\zeta\right)e^{in\theta}.$$

By substituting $g_j(\xi,\zeta)$ into the last relationship from (2.16), for $c < c_R$ one can obtain

$$\Phi_{j1} = \sum_{n=-\infty}^{\infty}\left(a_{nj}K_n(k_{j1}r) + b_{nj}I_n(k_{j1}r)\right)e^{in\theta}, \tag{2.18}$$

where $b_{nj} = \sum_{l=1}^{3}\sum_{m=-\infty}^{\infty}a_{ml}A_{nj}^{ml}$, $A_{nj}^{ml} = \int_{-\infty}^{\infty}\frac{\Delta_{jl}^*}{\Delta^*}\Phi_{ml}\Phi_{nj}e^{-h(f_l+f_j)}d\zeta$.

By substituting (2.18) at $k = 1$ and by substituting (2.12) at $k = 2$, into the relationships for u_{lk}^*, σ_{lmk}^* $(l,m = r,\theta,\eta)$, one can obtain new relationships for the SSS components for the body and for the aggregate in cylindrical coordinates at $c < c_R$, where only coefficients $a_{n1},\ldots,a_{n9}$ are unknown.

By substituting (2.10) into (2.2) and resolving the system of equations obtained for the nth term of expansion with respect $u_{0m\eta k}$, $u_{0n\theta k}$, u_{0nrk} one can find the corresponding expressions.

In order to determine coefficients $a_{n1},\ldots,a_{n9}$ let us use boundary conditions (2.4) or (2.5) rewritten for u_{lk}^* $(l = r,\theta,\eta)$ and $\sigma_{r\eta l}^*$, $\sigma_{r\theta l}^*$ depending on the conjugation condition between the shell and the body. By substituting the corresponding relationships into the boundary conditions and equating the coefficients of the series at $e^{in\theta}$, one can obtain an infinite system $(n = 0,\pm1,\pm2,\ldots)$ of linear algebraic equations that can be solved using a reduction method or the method of successive reflections being more convenient for solving the formulated problem [2], which makes it possible to solve for each successive reflection a block-diagonal system of linear equations, with 9×9 matrices and determinants $\Delta_n(\xi,c)$ along the main diagonal.

Knowing the solution of the problem for a sinusoidal load, the response of the shell and its environment with respect to an aperiodic (local) load moving at a constant velocity in the form of $P(\theta,\xi) = p(\theta)p(\eta)$ (characteristic of vehicles) can be found using superposition, based on the representation of the load and the body and aggregate SSS components in form of Fourier integrals, as it follows

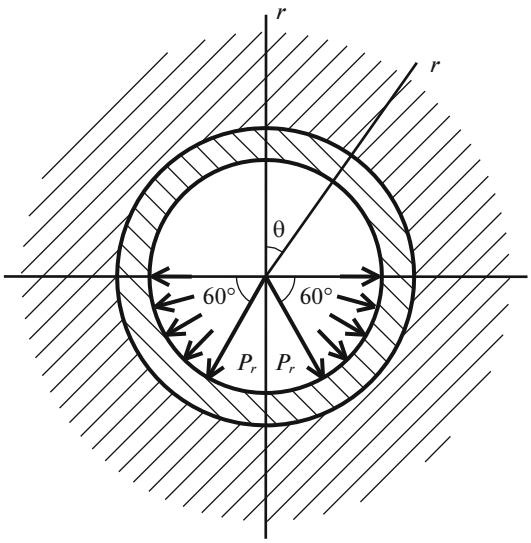

Fig. 2. A load moving along the tunnel tray.

Table 1. SSS components of the tunnel cross-section ($\eta = 0$) affected by a symmetric moving load

r	SSS component	θ, deg									
		0	20	40	60	80	100	120	140	160	180
			−20	40	−60	−80	−100	−120	−140	−160	
Aggregate (concrete layer)											
R_2	$u_r^\circ \times 10$	−0.25	−0.23	−0.17	−0.07	0.08	0.23	0.30	0.27	0.18	0.13
	$\sigma_{r\theta}^\circ$	0.0	0.15	0.17	0.12	0.07	0.0	−0.11	−0.15	−0.09	0.0
			−0.15	−0.17	−0.12	−0.07		0.11	0.15	0.09	
	$\sigma_{\theta\theta}^\circ$	0.02	0.10	0.29	0.45	0.34	0.02	−0.10	0.24	0.80	1.08
	$\sigma_{\eta\eta}^\circ$	−0.10	−0.16	−0.15	−0.13	−0.67	−1.72	−2.25	−1.61	−0.47	0.08
R_1	$u_r^\circ \times 10$	−0.24	−0.22	−0.17	−0.07	0.07	0.21	0.28	0.25	0.17	0.13
	$\sigma_{r\theta}^\circ$	0.0	0.04	0.04	0.05	0.10	0.10	−0.03	−0.02	−0.02	0.0
			−0.04	−0.04	−0.05	−0.10	−0.10	0.03	0.02	0.02	
	$\sigma_{\theta\theta}^\circ$	−0.09	−0.07	0.07	0.01	0.50	1.32	1.74	1.23	0.24	−0.25
	$\sigma_{\eta\eta}^\circ$	−0.54	−0.48	−0.35	−0.10	0.52	1.33	1.67	1.18	0.32	−0.10
Rock body											
R_1	$u_r^\circ \times 10$	−0.24	−0.22	−0.17	−0.07	0.07	0.21	0.28	0.25	0.17	0.13
	$\sigma_{r\theta}^\circ \times 10$	0.0	0.03	0.05	0.04	−0.02	−0.07	−0.08	−0.05	−0.02	0.0
			−0.03	−0.05	−0.04	0.02	0.07	0.08	0.05	0.02	
	$\sigma_{\theta\theta}^\circ \times 10$	−0.02	−0.02	0.01	0.05	0.05	−0.01	−0.06	−0.04	0.02	0.06
	$\sigma_{\eta\eta}^\circ \times 10$	−0.05	−0.04	−0.01	0.02	0.01	−0.01	−0.03	−0.01	0.02	0.04

Table 2. SSS components of the tunnel cross-section ($\eta = 0$) affected by an asymmetric moving load

r	SSS component	θ, deg									
		0	20	40	60	80	100	120	140	160	180
Aggregate (concrete layer)											
R_2	$u_r^\circ \times 10$	−0.38	−0.35	−0.28	−0.17	−0.02	0.13	0.21	0.20	0.16	0.20
	$\sigma_{r\theta}^\circ$	0.10	0.29	0.26	0.12	−0.01	−0.14	−0.21	−0.16	−0.03	0.11
	$\sigma_{\theta\theta}^\circ$	0.03	0.03	0.20	0.36	0.26	−0.03	−0.08	0.41	1.18	1.61
	$\sigma_{\eta\eta}^\circ$	−0.15	−0.28	−0.31	−0.28	−0.82	−1.83	−2.28	−1.63	−0.44	0.11
R_1	$u_r^\circ \times 10$	−0.36	−0.35	−0.29	−0.19	−0.04	0.11	0.19	0.18	0.15	0.19
	$\sigma_{r\theta\theta}^\circ$	0.03	0.09	0.08	0.06	0.07	0.05	−0.06	−0.19	−0.17	0.05
	$\sigma_{\theta\theta}^\circ$	−0.14	−0.06	0.02	0.14	0.60	1.35	1.71	1.16	0.81	−0.38
	$\sigma_{\eta\eta}^\circ$	−0.80	−0.64	−0.42	−0.12	0.47	1.19	1.43	0.89	0.05	−0.15
Rock body											
R_1	$u_r^\circ \times 10$	−0.36	−0.35	−0.29	−0.19	−0.04	0.11	0.19	0.18	0.15	0.19
	$\sigma_{r\theta}^\circ \times 10$	0.06	0.07	0.05	0.01	−0.03	−0.05	−0.10	−0.17	−0.15	0.01
	$\sigma_{\theta\theta}^\circ \times 10$	−0.01	0.0	0.02	0.03	0.0	−0.01	0.03	0.05	−0.02	−0.05
	$\sigma_{\eta\eta}^\circ \times 10$	−0.07	−0.06	−0.02	0.01	−0.01	−0.03	−0.02	0.01	0.02	0.02
r	SSS component	θ, deg									
		0	−20	−40	−60	−80	−100	−120	−140	−160	−180
Aggregate (concrete layer)											
R_2	$u_r^\circ \times 10$	−0.38	−0.33	−0.22	−0.02	0.26	0.56	0.71	0.61	0.38	0.20
	$\sigma_{r\theta}^\circ$	0.10	−0.16	−0.25	−0.23	−0.23	−0.14	0.11	0.30	0.26	0.11
	$\sigma_{\theta\theta}^\circ$	0.03	0.25	0.68	1.00	0.77	0.10	−0.22	0.32	1.23	1.61
	$\sigma_{\eta\eta}^\circ$	−0.15	−0.19	−0.13	−0.11	−1.18	−3.33	−4.46	−3.21	−0.97	0.11
R_1	$u_r^\circ \times 10$	−0.36	−0.32	−0.22	−0.03	0.24	0.52	0.66	0.57	0.36	0.19
	$\sigma_{r\theta\theta}^\circ$	0.03	−0.03	−0.03	−0.10	−0.26	−0.25	0.04	0.32	0.31	0.05
	$\sigma_{\theta\theta}^\circ$	−0.14	−0.15	−0.23	−0.11	0.91	2.63	3.50	2.52	0.63	−0.38
	$\sigma_{\eta\eta}^\circ$	−0.80	−0.80	−0.65	−0.17	1.09	2.80	3.59	2.66	0.90	−0.15
Rock body											
R_1	$u_r^\circ \times 10$	−0.36	−0.32	−0.22	−0.03	0.24	0.52	0.66	0.57	0.36	0.19
	$\sigma_{r\theta}^\circ \times 10$	0.06	0.02	−0.02	−0.03	−0.01	−0.01	0.03	0.12	0.14	0.01
	$\sigma_{\theta\theta}^\circ \times 10$	−0.01	−0.01	0.01	0.03	0.0	−0.04	−0.01	0.03	−0.01	−0.05
	$\sigma_{\eta\eta}^\circ \times 10$	−0.07	−0.05	−0.01	0.03	0.02	−0.03	−0.04	0.01	0.03	0.02

$$P(\theta,\eta) = \frac{1}{2\pi}\int_{-\infty}^{\infty} P^*(\theta,\xi)\,e^{i\xi\eta}d\xi = p(\theta)\,p(\eta) = p(\theta)\frac{1}{2\pi}\int_{-\infty}^{\infty} p^*(\xi)\,e^{i\xi\eta}d\xi,$$

$$P_m(\theta,\eta) = \frac{1}{2\pi}\int_{-\infty}^{\infty} P_m^*(\theta,\xi)\,e^{i\xi\eta}d\xi = p_m(\theta)\,p(\eta) = p_m(\theta)\frac{1}{2\pi}\int_{-\infty}^{\infty} p^*(\xi)\,e^{i\xi\eta}d\xi,$$

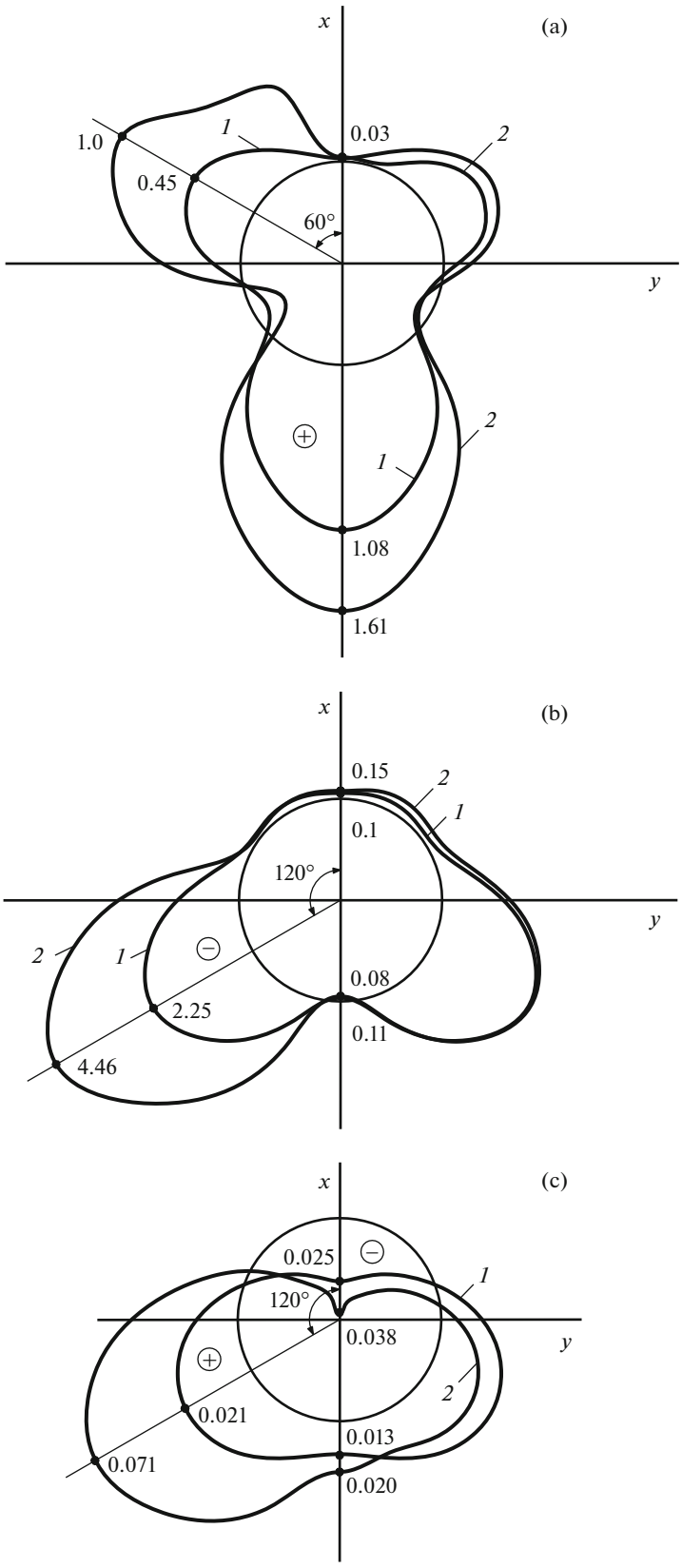

Fig. 3. Diagrams for stresses (a) $\sigma_{\theta\theta}$, (b) $\sigma_{\eta\eta}$ and displacements (c) u_r on the contour $r = R_2$ ($\eta = 0$) of the aggregate contact surface: (*1*) symmetric loading; (*2*) asymmetric loading.

Table 3. SSS components of Earth's surface in the *xy* plane ($\eta = 0$) under symmetric and asymmetric tunnel loading

SSS component	y/R										
	0.0	−0.2	−0.4	−0.6	−0.8	−1.0	−1.2	−1.4	−1.6	−1.8	−2.0
		0.2	0.4	0.6	0.8	1.0	1.2	1.4	1.6	1.8	2.0
Symmetric loading											
$u_x^\circ \times 10$	−0.24	−0.24	−0.23	−0.23	−0.23	−0.22	−0.22	−0.21	−0.21	−0.20	−0.20
$u_y^\circ \times 100$	0.0	0.04	0.07	0.09	0.11	0.12	0.12	0.11	0.10	0.08	0.07
		−0.04	−0.07	−0.09	−0.11	−0.12	−0.12	−0.11	−0.10	−0.08	−0.07
$\sigma_{yy}^\circ \times 100$	−0.42	−0.41	−0.37	−0.32	−0.26	−0.20	−0.15	−0.11	−0.08	−0.06	−0.06
$\sigma_{yy}^\circ \times 100$	−0.80	−0.79	−0.76	−0.72	−0.68	−0.63	−0.58	−0.54	−0.51	−0.49	−0.47
Asymmetric loading											
$u_x^\circ \times 10$	−0.36	−0.36	−0.36	−0.36	−0.35	−0.34	−0.33	−0.33	−0.32	−0.31	−0.30
		−0.35	−0.35	−0.34	−0.33	−0.32	−0.31	−0.31	−0.30	−0.30	−0.30
$u_y^\circ \times 10$	−0.17	−0.17	−0.16	−0.15	−0.15	−0.14	−0.14	−0.14	−0.14	−0.14	−0.15
		−0.18	−0.18	−0.18	−0.18	−0.18	−0.18	−0.18	−0.17	−0.17	−0.17
$u_{yy}^\circ \times 100$	−0.67	−0.71	−0.70	−0.64	−0.55	−0.44	−0.33	−0.23	−0.15	−0.10	−0.06
		−0.58	−0.46	−0.33	−0.22	−0.14	−0.08	−0.05	−0.05	−0.06	−0.08
$\sigma_{\eta\eta}^\circ \times 100$	−1.22	−1.24	−1.22	−1.18	−1.11	−1.03	−0.95	−0.87	−0.80	−0.74	−0.70
		−1.16	−1.09	−1.00	−0.92	−0.85	−0.78	−0.74	−0.71	−0.69	−0.68

$$m = r, \theta, \eta; \tag{2.19}$$

$$u_{lk}(r,\theta,\eta) = \frac{1}{2\pi}\int_{-\infty}^{\infty} u_{lk}^*(r,\theta,\xi)p^*(\xi)\,d\xi, \quad \sigma_{lmk}(r,\theta,\eta) = \frac{1}{2\pi}\int_{-\infty}^{\infty} \sigma_{lmk}^*(r,\theta,\xi)p^*(\xi)\,d\xi,$$

$$l = r, \theta, \eta, \quad m = r, \theta, \eta, \quad k = 1, 2.$$

Here, $p^*(\xi) = \int_{-\infty}^{\infty} p(\eta)e^{-i\xi\eta}d\eta$.

In order to calculate displacements and stresses (2.19), any numerical integration method can be used if determinants $\Delta_n(\xi, c)$ ($n = 0, \pm1, \pm2, \ldots$) differ from zero, i.e., when load motion velocity c is less than critical velocities $c_{(n)^*}$. The values of $c_{(n)^*}$ can be determined based on dispersion equations $\Delta_n(\xi, c) = 0$ [3] and could be lower than the Rayleigh velocity. The final solution should depend on the specific type of moving load.

It should be noted that excluding boundary conditions (2.3) from the problem formulation and excluding $\Phi_{j1}^{(2)}$ from (2.12), one can obtain a solution of a similar problem for an elastic space.

3. NUMERICAL EXPERIMENTS

Let us consider a tunnel reinforced by a three-layer lining with depth $h = 6$ m in a rock body with the following characteristics: $\nu_1 = 0.294$, $\mu_1 = \mu = 1.094 \times 10^8$ Pa, $\rho_1 = 1.5 \times 10^3$ kg/m^3. Design parameters for lining: the sheathing consists of thin-walled steel shells ($\nu_{01} = \nu_{02} = 0.3$, $\mu_{01} = \mu_{02} = 8.08 \times 10^{10}$ Pa, $\rho_{01} = \rho_{02} = 7.8 \times 10^3$ kg/m^3) having the same thickness $h_{01} = h_{02} = 0.02$ m with median surface radii

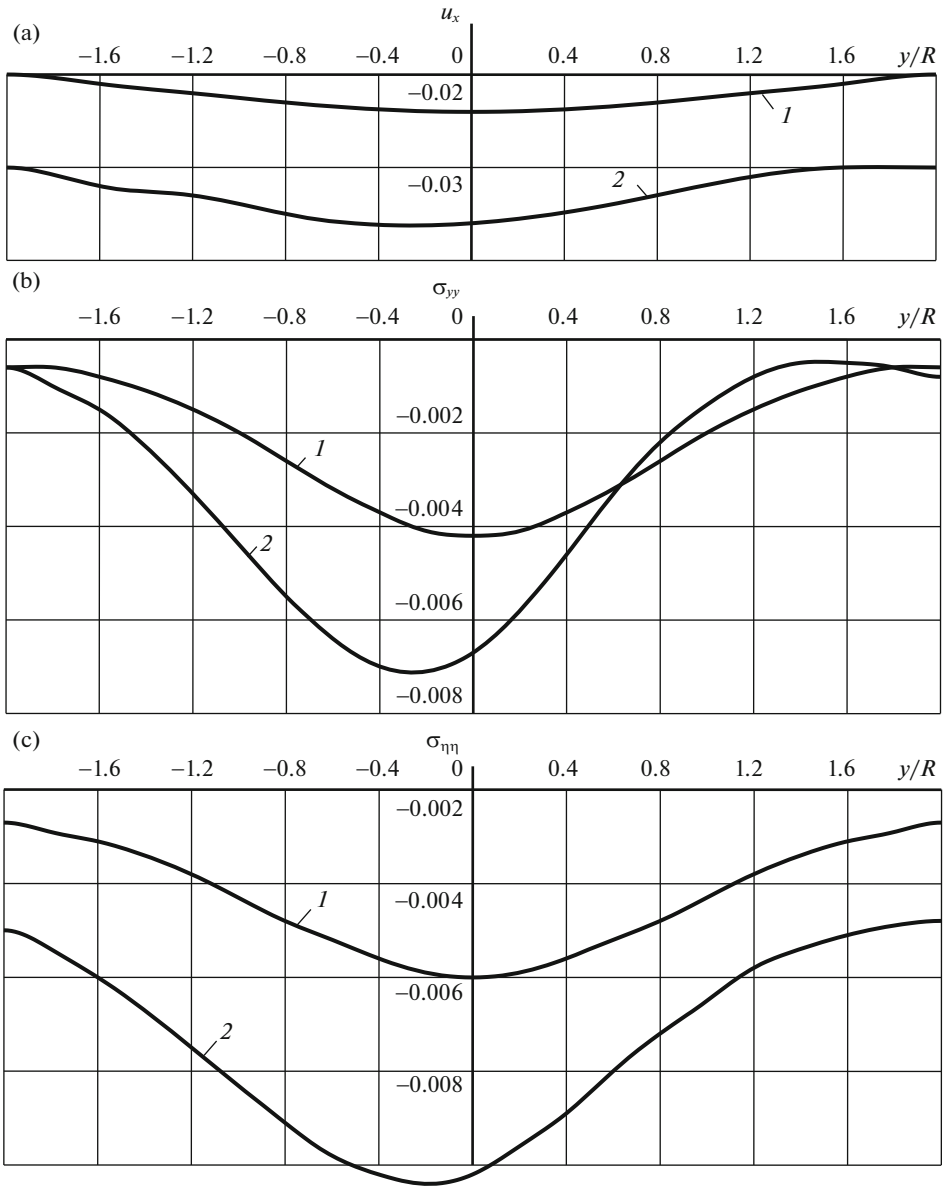

Fig. 4. Changes in the SSS components of Earth's surface in the *xy* plane.

$R_1 = 3.0$ m and $R_2 = 2.5$ m; aggregate represents a thick-walled concrete shell ($\nu_2 = 0.2$, $\mu_2 = 1.21 \times 10^{10}$ Pa, $\rho_2 = 2.5 \times 10^3$ kg/m^3). The contact between the rock body and the lining, as well as that between the lining layers is assumed rigid.

Let us investigate the stress-strain state of the considered tunnel under consideration affected by the cylindrical normal load originating from intra-tunnel transport moving along its tray at a velocity of 100 m/s (see Fig. 2). The load is uniformly distributed along the η axis in the range of $|\eta| \le l_0 = 0.2$ m.

Let us consider the two cases of loading: symmetric and asymmetric. In the first case, it is considered that the intensity of the load is constant throughout the entire surface of the load application, that is, $P_r = q$.

In the second case, the intensity of the load located to the left of the vertical diametral plane of the tunnel uniformly distributed throughout the angular coordinate is twice the intensity of the same load that acts to the right of this plane, that is, at $90° \le \theta \le 150°$ $P_r = q$; at $210° \le \theta \le 270°$ $P_r = 2q$.

Load parameter q (Pa) is chosen in such a way that the total load along the entire length of the loading section ($2l_0$, m) amounts to the equivalent concentrated normal ring load with intensity $P^{\circ\circ}$ (N/m), i.e., $q = P/2l_0$.

The numerical studies on the dispersion equations corresponding to this case have shown that these equations have no roots in the subsonic velocity range.

Let us introduce the following notations: $u_r^\circ = u_r\mu/P^\circ$ (m), (m), $\sigma_{r\theta}^\circ = \sigma_{r\theta}/P^\circ$, $\sigma_{\theta\theta}^\circ = \sigma_{\theta\theta}/P^\circ$, $\sigma_{\eta\eta}^\circ = \sigma_{\eta\eta}/P^\circ$, $u_x^\circ = u_x\mu/P^\circ$ (m), (m), $u_y^\circ = u_y\mu/P^\circ$ (m), $\sigma_{yy}^\circ = \sigma_{yy}/P^\circ$, where $P^\circ = P^{\circ\circ}/\text{m}$ (Pa).

Tables 1 and 2 contain the calculation data for the SSS of the tunnel cross section ($\eta = 0$) affected by a symmetric and asymmetric moving load.

According to data presented in Tables 1 and 2, Fig. 3 shows the diagrams of normal stresses $\sigma_{\theta\theta}^\circ$, $\sigma_{\eta\eta}^\circ$ and radial displacements u_r° along contour $r = R_2$ of the contact with the inner shell of the concrete layer sheathing at $\eta = 0$.

From the analysis of the calculation results it follows that in the case of an asymmetric load, i.e., when the intensity of the left half of the symmetric load exhibits a two-fold increase, the symmetric character of displacement and stress distribution along the contours of the tunnel cross-section is violated. At the same time, in the aggregate (concrete layer), extreme radial displacements u_r at $\theta = -120°$ exhibit a 3.4-fold increase, whereas extreme stresses $\sigma_{r\theta}$, $\sigma_{\theta\theta}$, and $\sigma_{\eta\eta}$ exhibit a 2.0-fold increase (at $\theta = -140°$), a 1.5-fold increase (at $\theta = 180°$), and a 2.0-fold increase (at $\theta = -120°$), respectively. On the surface of the body contacting the lining, under any loading of the tunnel, the extreme stresses are much lower than for the concrete layer of the lining.

On Earth's surface, the symmetry in the distribution of stresses and displacements is violated, too. The results of SSS calculations for Earth's surface in coordinate plane xy ($\eta = 0$) affected by a symmetric and asymmetric moving load on the tunnel are presented in Table 3.

Figure 4 shows in the coordinate plane xy ($\eta = 0$) the changes in the SSS components of Earth's surface affected by symmetric and asymmetric moving loads on the tunnel. Designation of the curves is (curve *1*) for the symmetric loading and (curve *2*) for the asymmetric loading. As it follows from the analysis of the calculation results, in the second case of loading (under asymmetric loading), the maximum Earth's surface deflection u_x is 1.5 times greater than it is in the first case (under symmetric loading), whereas its maximum horizontal displacement u_y exhibits a 15-fold increase. Extreme normal stresses σ_y and $\sigma_{\eta\eta}$ increase by the factors of 1.7 and 1.5, respectively.

CONCLUSIONS

The obtained solution and the software package developed based on it makes it possible to use mathematical simulation methods for studying the dynamics of the rock body and its surface along the tunnel route at different depths, taking into account the physicomechanical properties of the body and the material of the lining structural elements. The motion velocity of the transport load significantly affects the dynamics of the surface of the body, which should be taken into account, for example, in the construction of subways, especially nowadays in connection with the intensive development of high-velocity rail transport. The choice of the material and thickness for the shell layers in the tunnel lining makes it possible to reduce the vibration of the body surface along the route negatively affecting the seismic stability of buildings and structures located nearby.

It should be also noted that the velocities of modern vehicles are in the range of subsonic velocities considered here and are much lower than the upper limit.

REFERENCES

1. Zh. S. Erzhanov, Sh. Aitaliev, and L. A. Alekseyeva, *Dynamics of Tunnels and Underground Pipelines* (Nauka, Alma-Ata, 1989) [in Russian].
2. V. N. Ukrainets, *Dynamics of Shallow Tunnels and Underground Pipelines under Moving Loads* (PSU Publ., Pavlodar, 2006) [in Russian].
3. L. A. Alekseyeva and V. N. Ukrainets, "Dynamics of an elastic half-space with a reinforced cylindrical cavity under moving loads," Int. Appl. Mech **45** (9), 75–85 (2009).

4. V. N. Ukrainets and S. R. Girnis, *Mathematical Modeling of the Dynamics of Tunnels Supported by Two-Layer Shells under the Action of Transport Loads* (Kereku Publ., Pavlodar, 2018) [in Russian].
5. İ. Coşkun and D. Dolmaseven, "Dynamic response of a circular tunnel in an elastic half space," J. Eng., art. id 6145375 (2017).
https://doi.org/10.1155/2017/6145375
6. J. P. Dwivedia, V. P. Singha, R. K. Lalb, and S. Devia, "Dynamic response of lined circular tunnel in linear viscoelastic medium due to moving ring load," Mater. Today: Proc. **4** (2), Pt. A, 3767–3775 (2017).
7. Z. Cao, S. Sun, Z. Yuan, and Y. Cai, "Analytical study on the effect of moving surface load on underground tunnel," in *Proc. China-Europe Conf. on Geotechnical Engineering,* Ed. by W. Wu and H. S. Yu (Springer, Cham, 2018).
8. Shunhua Zhou, *Dynamics of Rail Transit Tunnel Systems* (Acad. Press, London, 2019).

Translated by O. Polyakov